3D imaging and wavefront sensing with a plenoptic objective

J.M. Rodríguez-Ramos*[a], J.P. Lüke[a], R. López [b], J.G. Marichal-Hernández[a], I. Montilla[b], J. Trujillo-Sevilla[a], B. Femenía[b], M. Puga[a], M. López[a], J.J. Fernández-Valdivia[a], F. Rosa[a], C. Dominguez-Conde[a], J.C. Sanluis[a], L.F. Rodríguez-Ramos[b]

[a]Universidad de La Laguna, Canary Islands, Spain.
[b]Instituto de Astrofísica de Canarias, Canary Islands, Spain.

ABSTRACT

Plenoptic cameras have been developed over the last years as a passive method for 3d scanning. Several superresolution algorithms have been proposed in order to increase the resolution decrease associated with lightfield acquisition with a microlenses array. A number of multiview stereo algorithms have also been applied in order to extract depth information from plenoptic frames. Real time systems have been implemented using specialized hardware as Graphical Processing Units (GPUs) and Field Programmable Gates Arrays (FPGAs).

In this paper, we will present our own implementations related with the aforementioned aspects but also two new developments consisting of a portable plenoptic objective to transform every conventional 2d camera in a 3D CAFADIS plenoptic camera, and the novel use of a plenoptic camera as a wavefront phase sensor for adaptive optics (OA).

The terrestrial atmosphere degrades the telescope images due to the diffraction index changes associated with the turbulence. These changes require a high speed processing that justify the use of GPUs and FPGAs. Na artificial Laser Guide Stars (Na-LGS, 90km high) must be used to obtain the reference wavefront phase and the Optical Transfer Function of the system, but they are affected by defocus because of the finite distance to the telescope. Using the telescope as a plenoptic camera allows us to correct the defocus and to recover the wavefront phase tomographically.

These advances significantly increase the versatility of the plenoptic camera, and provides a new contribution to relate the wave optics and computer vision fields, as many authors claim.

Keywords: CAFADIS, plenoptic, wavefront, lightfield, adaptive optics, 3D, GPU, FPGA

1. INTRODUCTION

Plenoptic cameras have been developed over the last years as a passive method for the 3D understanding of a scene. A conventional camera makes use of a convergent lens in order to concentrate a bunch of rays coming from sharp points in the scene into a single pixel in the sensor. Focusing/defocusing is the price to pay to gather more light. A plenoptic camera separates part of those rays that were to be integrated into one pixel, in bunches of rays that come from the same position of the scene, but with different angular directions by the use of a microlenses array. To record them a trade-off must be done to observe simultaneously the angular and positional structure of light coming from the scene.

Until now, the most common treatment for plenoptic images consists of applying multistereo computer vision techniques, considering that there are as many points of views as there are pixels behind each microlens. Nevertheless, an alternative procedure, that turns out to be efficient, as well as complementary in fields like Adaptive Optics for Astrophysics, employs plenoptic cameras as tomographic wavefront phase sensors. The double treatment we are proposing is in accordance with the wish of several authors who claim to use computer vision tools to solve wave optics problems and viceversa.

*jmramos@ull.es; phone +34 922 318 249; fax +34 922 318 228;

Within a plenoptic frame there is enough information to recreate *a posteriori* a volume of images covering a range of focusing distances, what is known as a focal stack. Attending to a measure of focusing through each ray that crosses that volume it is possible to estimate distances to objects. Algorithms have been developed to tackle all of these processes at video acquisition rate and nowadays it is possible to build around these methods a 3D camera, even one suitable to feed a glasses free 3D display. For the sake of speed parallel hardware is usually employed in the form of Graphics Processing Units and Field Programmable Gates Arrays.

Plenoptic methods, of course, have their inconveniences. The valid range of refocusing distances is constrained by the number of pixels that contribute to gather angular information. Moreover the specific placement of centres of depth of field of the resulting images is far from being linear, and is best suited for filming on close distances, which incidentally are a hard task when using stereo techniques. If we increment the number of angular pixels there are less remaining pixels to gather "positional" resolution. This sacrifice can not be fully overcome, but can be diminished by the use of superresolution methods. Also, when the microlenses array is placed close to the sensor, it is hard to avoid a certain tilt between them. This is the reason that explains the calibration stage that is mandatory previous to any further processing.

CAFADIS, the plenoptic camera patented by the University of La Laguna (Rodríguez-Ramos *et al.* [1]), brings several advantages with respect to previous methods in this field: a new calibration method for plenoptic frames that can be computed in real time (section 2), a superresolution algorithm (section 3) and a construction design of plenoptic interchangeable objectives (section 4).

There are fields were the plenoptic sensor can be used in two senses at the same time: depth extraction and tomographic wavefront sensing. The terrestrial atmosphere degrades the telescope images due to the diffraction index changes associated to the turbulence. These changes require the high speed processing supplied by the GPUs and the FPGAs. Na artificial Laser Guide Stars (Na-LGS, 90km high) must be used to obtain the reference wavefront phase and the Optical Transfer Function of the system, but they are affected by defocus because of the finite distance to the telescope. Using the telescope as a plenoptic camera allows us to correct the defocus and to recover the wavefront phase tomographically (Rodríguez-Ramos *et al* [2]) (section 5).

2. PLENOPTIC FRAME CALIBRATION

The physical manufacturing of a plenoptic camera requires to locate the microlenses array somehow aligned with the imaging sensor. Perfect alignment is very difficult to obtain and pixel and microlens pitches will not be exact multiples in a general case, thus some sort of calibration is needed previous to any image rearrangement, in order to identify the relative position of every subpupil image on the detector.

Using the rather accurate nature of the manufacturing processes of both the imaging sensor and the microlenses array, we will consider them as “perfect”, and thus uniquely identified by their respective pitches, i.e., 7.4 microns per pixel at the detector and 400 microns per microlens at the microlens array. Within this framework, the manufacturing process of the plenoptic camera will be modelled as a combination of a scale change, a rotation and a displacement, and quantitatively described by:

- The imaged microlens pitch: The combination of the microlens pitch and the scale change due to the imaging system. It can also be associated with the microlens pitch measured in pixels.
- The relative rotation: The angular orientation between the pixel and the microlens axes.
- The lateral displacement: Some sort of vertical and horizontal bias to be considered in order to obtain the relative position of the microlenses with respect to the imaging sensor.

These four parameters are considered the result of the calibration and completely describe the result of the manufacturing process under the written assumptions. A number of methods were used to obtain these parameters.

2.1 Aperture reduction.

The aperture reduction method consists in the evaluation of a specifically obtained image with a reduced pupil size. The pupil is reduced by manually closing the iris in a way in which only the aperture centres are illuminated. Provided that the angular misalignment is less than one microlens at the edge of the imaging sensor, the following algorithm can be used with very accurate results. It is also recommended to use a flat image scene, although not strictly necessary.

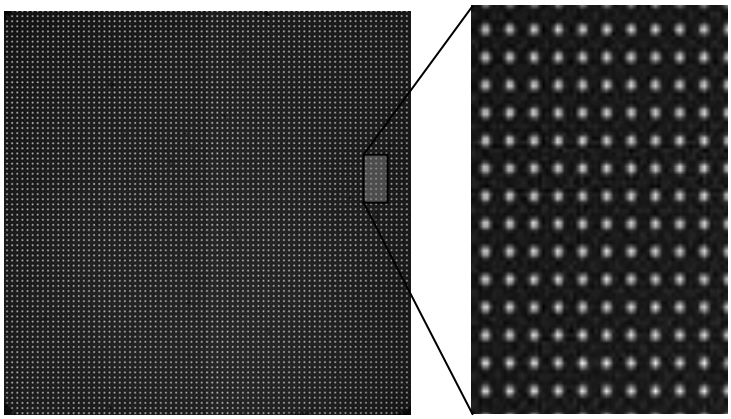

Figure 1. Left: plenoptic frame with aperture-reduced acquisition. Right: plenoptic frame section zoomed.

The Figure 1 shows an aperture-reduced image of a uniform scene, showing illumination only at the centres of the microlenses. The first step is to compute an approximate value for the pitch, using a two-dimensional Fourier transform which shows very sharp spikes at the microlens pitch expressed in pixels. Five lines are combined to improve peak capture and the first spike is identified in both horizontal and vertical orientations. The average value is used as a first estimation of the pitch.

Second step is to draw a reticule using the estimated pitch plus one of the maximum values located the centre of the image, in order to approximately identify all the microlenses.

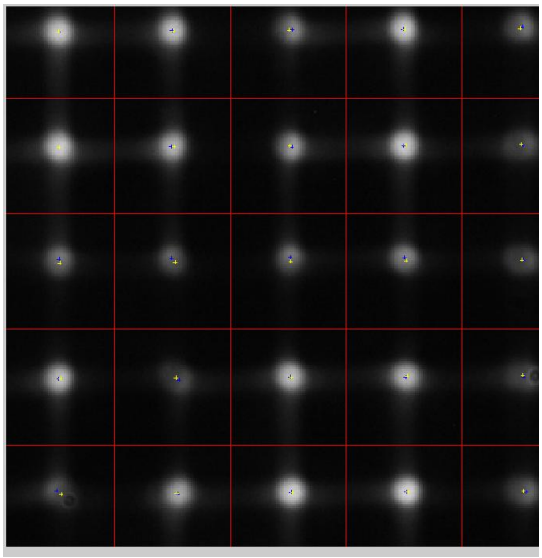

Figure 2. Resulting centres as yellow crosses.

Third step is to compute the centre of gravity of the light existing within every microlens, which provides a reasonable estimation of the geometrical centre of the microlens.

The forth and final step is to compute a blind minimization adjusting the computed gravity centres to a model containing only the four parameter of the calibration: microlenses pitch, rotation angle, horizontal and vertical displacement. The values found are the ones which minimise the quadratic distance from all the computed gravity centres to the ones resulting from the model. The resulting centres are drawn as yellow crosses in Figure 2, and will be regularly spaced and aligned as implied by the model, thus correcting local displacements due to either microlens and/or detector local defects, as shown in the lower left microlens of the Figure 2.

2.2 Two-dimensional Fourier Transform.

The aperture reduction method requires a specific setup for the camera and imposes a limit in the relative rotation. These are significant drawbacks that should be removed using alternative calibration methods for a general case, even accepting the compromise of less accuracy.

The direct estimation of both pitch and rotation from the two-dimensional Fourier transform is feasible provided that a Blackmann-Harris windowing is performed on the plenoptic image (see Gasior & González[3]), and a four-times zero-padding scheme is used to interpolate in order to estimate the frequency peak with the required resolution. Rotation is estimated from the angle between positive and negative spikes of the two-dimensional Fourier transform.

2.3 Lateral displacement computation using linear correlation.

Fourier transform method previously described provides a very reasonable measurement for both the microlens pitch and angular rotation. However they are not very accurate when computing the lateral displacement or "phase" of the calibration.

Once that pitch and rotation have been measured, the lateral displacement identification aims to locate the centre of one of the microlenses, because doing so all of them can be obtained from the model. Three methods have been tested for this purpose. A first approach is to use the cross-correlation technique with only one line of the image, instead of using the whole image. This shortage greatly reduces the computational cost.

2.4 Lateral displacement computation using correlation.

This method is based in the fact that the illumination at the centre of the microlens is, on average, greater than on the periphery. Under this assumption, a simulated plenoptic image can be generated using a sinusoidal profile in both vertical and horizontal axes, using the measured pitch and rotation.

The simulated image is cross-correlated with the original one, after suppression of the zero frequency component, and lower frequencies if needed, expecting to found a maximum at the lateral displacements in which both images better fit. Further quadratic interpolation may be used to precisely compute the displacement with sub-pixel resolution.

2.5 Lateral displacement computation using direct phase detection.

The correlation method previously described unfortunately requires a high computational cost associated with the cross-correlation. A simpler method based on the direct detection of phase could also be used, especially when real-time calibrations will be needed. The algorithm is based on the trigonometrical identity for the sum of two angles.

When the phases are very similar, the difference term will be very close to half that difference, and the adding term will generate twice the frequency that can be filtered out somehow, or be considered null provided that an integer number of wavelengths are involved.

2.6 Calibration methods benchmark.

A statistical study has been carried in order to compare the three methods. Correlation methods exhibit very good results.

Table 1. Absolute error in displacement computation.

Input image size	Method	Average error	Standard deviation
512x512	**Linear correlation**	0.5319	0.2951
	Bidimensional correlation	0.2957	0.1333
	Direct Detection	1.0673	0.7187
1024x1024	**Linear correlation**	0.2133	0.1356
	Bidimensional correlation	0.2254	0.0797
	Direct detection	1.2129	0.8128
2048x2048	**Linear correlation**	0.1952	0.1438
	Bidimensional Correlation	0.1051	0.0498
	Direct Detection	1.1374	0.8849

3. REFOCUSING METHODS WITH SUPERESOLUTION.

One of the disadvantages of plenoptic cameras is that the spatial resolution must decrease as a trade-off to accommodate, on the same sensor real-state, the pixels devoted to acquiring angular information. On this section two methods are described to alleviate this compromise: they get as many pixels on the resulting images, as there were on the original one. With this method in mind, the second one allows to generate simultaneously different refocusing distances as well as point of views, so it is suited to convert plenoptic sensor in a 3D stereoscopic camera.

3.1 Refocusing method that generates as many pixels as there were in the input image.

Let's consider an image acquired by a plenoptic camera where the microlens array contains N_y rows and N_x colums of identical microlenses within. All the microlenses have the same focal length *f*, and the image formed by the microlenses is acquired with a sensor perpendicular to the optical axis at distance *f* behind the microlenses. Each image formed behind a microlens occupies M times M pixels. Therefore the image as a whole can be considered as a digital signal with 4 parameters, *L(x, y, u, v)*, with *x* varying on the range [0, N_x-1], *y* on [0, N_y-1], *u* on [0, M-1], and *v* on [0, M-1].

Sampling is assumed to be regular on microlenses and pixels dimensions. The number of pixels after a microlens, M, must be a prime number, or a multiple of a prime number if several points of view are to be generated simultaneously.

It is known[4-7] that it is possible to recreate images with varying depth of focus starting from the same plenoptic image by solving the following integral:

$$\hat{I}_\alpha(x', y') = \iint \hat{L}\left(u\left(1-\tfrac{1}{\alpha}\right)+\tfrac{x'}{\alpha}, v\left(1-\tfrac{1}{\alpha}\right)+\tfrac{y'}{\alpha}, u, v\right) du\, dv \qquad (1)$$

$\hat{I}$ and $\hat{L}$ denote the continuous versions of the image and the plenoptic signal. It is usual, with illustrative means, to refer to a 2D plenoptic function, where parameters y and v are not taken into account. In that case the aforementioned integral becomes a line integral over a 2D space.

However this integral over a continuous signal must be modified according to the discrete nature of what can be acquired with a plenoptic digital camera. Our proposed method uses a discretization approach that differs from that previously reported on literature. We will introduce it with the aid of some figures.

Let's consider the scheme on Figure 3. Each rectangle on the scheme represents what is sensed within a single pixel of the whole sensor. We consider that each pixel accounts for an area of the space (x,u), instead of just a infinitesimal point, as usually assumed by other authors. This area covers the light that crosses the surface of a microlens, on axis x, and the several angular directions that emerge from the surface of the pixel, on axis u. We show the case N_x = 5 and M = 5.

On the scheme it is highligthed the projection of pixels behind a certain microlens, x_0. The projection is tilted in such a way that the upper left corner of the area of pixel (x_0, M-1), is projected onto lower left corner of pixel (x_0-k, 0). The Figure 3 illustrates the case x_0=1 and k = 1.

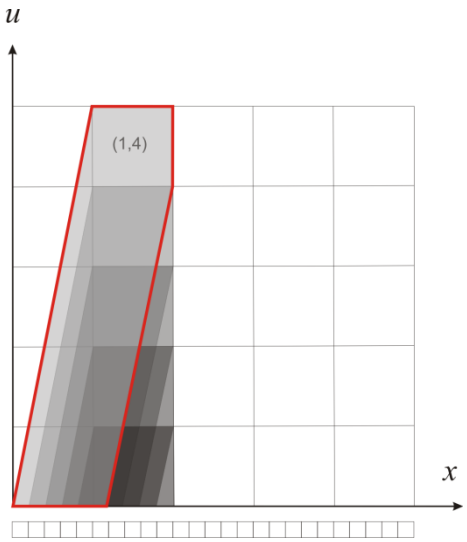

Figure 3. Pixels as area covering the space *(x, u)* and projection of each pixel on microlens 1 onto *x* axis.

We can see that if we project all the samples of the plenoptic function pertaining to microlens x_0=1, that is, the pixels (1, M-1), (1, M-2), … (1,0) a set of M strips appear on the x axis. If we integrate the areas covered by those strips on the plenoptic signal we would possibly obtain different values for each one. If we project all the samples of the discrete plenoptic signal in that way we would generate $N_x \cdot M$ different values that can be considered to form an image refocused at a distance that is associated with the slope value k. This image will have the same number of pixels that the sensor used to acquire the plenoptic signal, whatever value of k is used inside the range –M+1 … M-1 excluding 0.

On Figure 4 we show the strips of integration for all the possible slopes in the case M=5. That is k=-4,…,-1 as well as k=1, …,4. We show N_x=9 microlenses, instead of 5, just to accomodate the extra slopes. If we process all the strips using all the possible slopes we would obtain a set of images with different depths of focus. For a plenoptic signal with M pixels behind each microlens we can obtain 2M-2 images at different depths of focus.

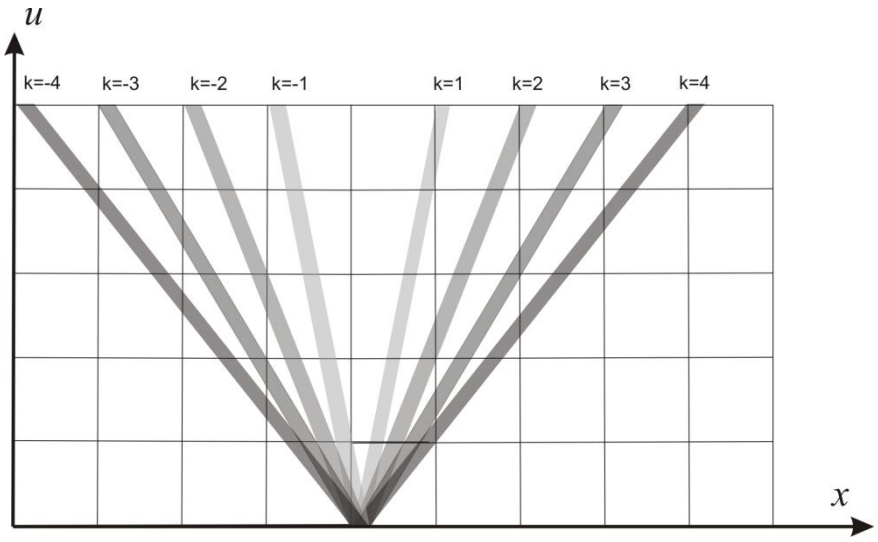

Figure 4. All the possible strips (with their associated slope) that project onto the same final pixel.

3.2 Refocusing method that simultaneously creates images with different points of view.

We can create d^2 images with different points of view, slightly displaced in horizontal and/or in vertical, if we use a number of pixels behind a microlens such that M/d is a prime number and we apply the previously described method d^2 times, considering each time just a $1/d^2$ portion of the pixels on the plenoptic image. Now, the slopes can vary on the range [-M/d+1…-1] and [1…M/d-1]. This implies that for each one of the d^2 resulting images with differents point of view there would be 2M/d-2 different depth of focus. Each image will have a size of $N_y \cdot M/d$ times $Nx \cdot M/d$ pixels.

Regarding with wich portion of the plenoptic image should be used for each point of view, lets see it with an example where d=2. In that case we are generating 4 different images, each one with a slightly different point of view. The first one considers only those pixels after microlens where p_x parameter varies between 0 and M/2-1, at the same time we cover with p_y the range between 0 and M/2-1; another image would be obtained considering p_x values between M/2 y M-1 while p_y varies between 0 and M/2-1; a third one would evaluate p_x between 0 and M/2-1, at the same time that p_y covers the range between M/2 and M-1; at last, p_x would vary between M/2 and M-1, whilst p_y varies between M/2 and M-1.

On the left side of Figure 5 it is shown the effect of considering apart the two halves of the pixels behind a microlens vertically or horizontally, on the right it is shown the four quarters of the main lens that contribute to different point of view when the division is made simultaneously on p_x and p_y.

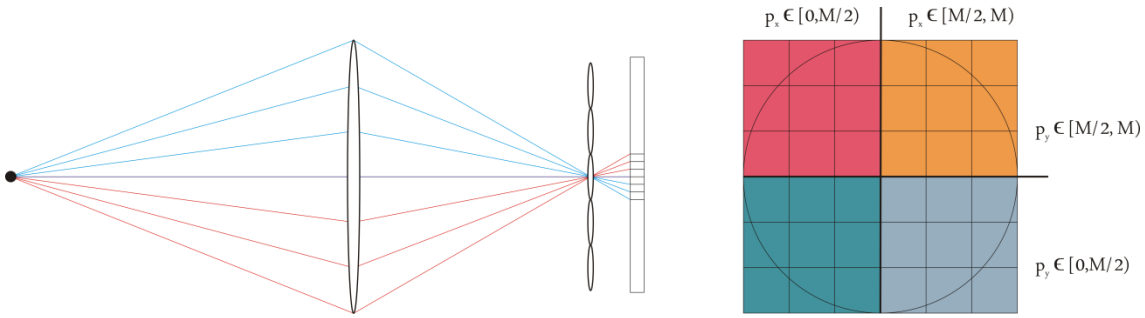

Figure 5. Left: division of pixels behind a microlens on two halves. Right: the 4 quarters with varying points of view that divide the main lens when we consider simultaneously a vertical and horizontal split.

The resulting images exhibit ¼ the size of the original plenoptic image. They can be combined to form just 2 images. For example blending the upper and lower point of views to the right and to doing the same with upper and lower views to the left we would obtain a stereoscopic pair.

An example of the image quality that proposed methods can deliver is shown in Figure 6. More examples, including videos, can be reached on a dedicated website[8].

4. INTERCHANGEABLE PLENOPTIC OBJECTIVE.

Until now, one of the greatest limitations to the use of plenoptic technology is the difficulties involved in its proper manufacturing. The manufacturing technique of the individual components is largely evolved: the objective lens, the detector even the microlenses array. But it is not easy to place, with the required accuracy, the microlenses array with respect to the sensor and the main lens. Sensors usually are protected with protective filters very close to them, in the order of a millimeter. To place the microlenses with a focal length within that range forces to use a very narrow field of view.

In order to get a wide field of view, f/numbers in the order of f/1.4 to f/2.8 should be chosen and therefore the microlenses array should be placed just micrometers apart from the sensor. To avoid this limitation is why we have

designed and implemented a plenoptic interchangeable objective that converts any conventional, single-body single-lens camera, into a 3 dimensional one.

This plenoptic objective system is composed by, at first stage, a refractive microlenses array; at a second stage, the images formed by such a multisystem are collected with an imaging optical vehicle, working in near field, once the incident beam is collimated; at last, it is collected by an optical element working conjugated to infinity that projects the set of images over the sensor.

The optic system has been miniaturized down to 10 centimeters and built as interchangeable using F-nikon mount, but a number of adapters allow to use it with different mounts: c-mount, micro 4/3, … Photographers or cameramen can continue to use their own objectives and cameras, and place our plenoptic objective in between to acquire plenoptic frames, then having access to the plenoptic technology: focal stack, 3D stereo focal stack (Figure 6), autostereoscopic images, depth maps and all-in focus images.

Figure 6. A pair of stereo images digitally focused at two different depths with our technology.

Our first HD 3D video results can be accessed online[8], the plenoptic objective is shown in there. From the same plenoptic video, several 3d stereo films can be generated, each one focused on a different plane. The focused plane can be changed even frame by frame. The rest of the planes are defocused. A RedOne cinema camera was used as detector, because its ability to record 4480 (h) x 2304 (v) in real time. Part of the bidimensional information recorded by so big sensor is converted in 3D information thanks to the optical plenoptic arrangement, and even HD stereo frames can be generated, enough quality for actual displays.

5. PLENOPTIC WAVEFRONT SENSOR

In Adaptive Optics (AO) all the plenoptic capabilities can be exploited at the same time (Figure 7). The most salient feature of our CAFADIS camera is its ability to simultaneously measuring wavefront maps and distances to objects[9]. This makes of CAFADIS an interesting alternative for LGS-based AO systems as it is capable of measuring from an LGS-beacon the atmospheric turbulence wavefront and simultaneously the distance to the LGS beacon thus removing the need of a NGS defocus sensor to probe changes in distance to the LGS beacon due to drifts of the mesospheric Na layer. In principle, the concept can also be employed to recover 3D profiles of the Na Layer allowing for optimizations of the measurement of the distance to the LGS-beacon.

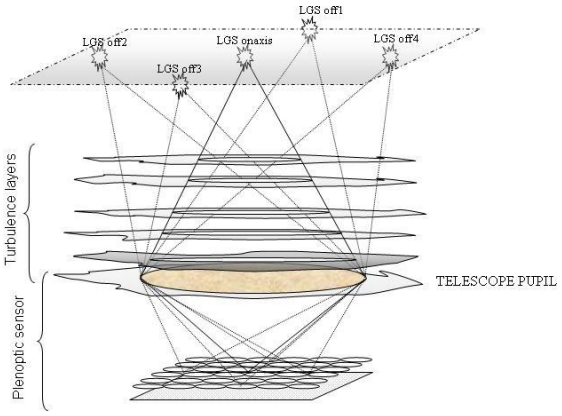

Figure 7. A LGS beacon system and six different turbulent layers are generated using CAOS. The cumulative wavefront phases at pupil plane, from each point of view, are calculated and retrieved with a plenoptic detector.

3.3 LGS beacon distance and Na Layer profiles.

For depth extraction the plenoptic sensor acts as a multiview stereo system, then the height variations of the LGS beacons, i.e. the information from the planes at different heights in the Na layer, is retrieved. This provides real-time information on the Na layer profile that can be introduced in the reconstruction algorithm to solve the problems derived by the spot elongation. Also we can compute at which height is focused the LGS. In Figure 8 we have plotted how using a plenoptic sensor we can scan the height from 70 km to 120 km for a 42 m telescope.

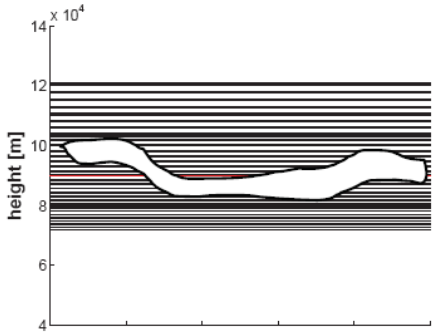

Figure 8. When conjugating the plenoptic detector to a plane at 90 km height, all the information from the planes around that height is retrieved and the height at which the LGS is focused can be recovered. From Montilla *et al.*[10]

3.4 Tomographic wavefront sensor.

The use of plenoptic optics for wavefront measurement was described by Clare and Lane[11] for the case of point sources. For wavefront phase extraction, it can be understood as a global sensor containing as extreme cases the Shack- Hartmann sensor and the pyramid sensor (2x2 microlenses array at telescope focus). The tomographic capability of the plenoptic sensors was demonstrated by Rodríguez-Ramos *et al.*[2]. They are especially adequate for computing the tomography of the atmospheric turbulence, as shown in Figure 9.

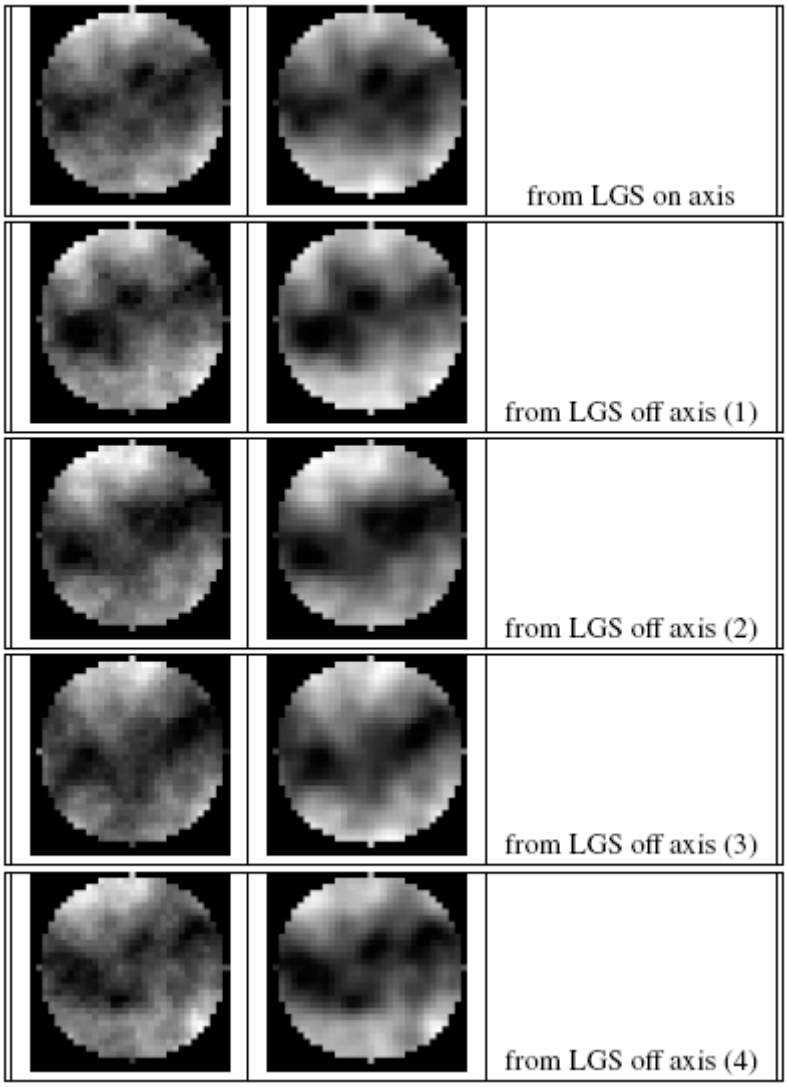

Figure 9. Simulation of the cumulative wavefront phases at the telescope pupil in five different points of view. Left column: original wavefront phases. Right column: recovered wavefront phases. Tilt has been removed in all the frames.

3.5 Multi-Conjugate Adaptive Optics (MCAO)

Multi-Conjugate Adaptive Optics (MCAO) will play a key role in future astronomy. Every Extremely Large Telescope (ELT) is being designed with its MCAO module, and most of their instruments will rely on that kind of correction for their optimum performance. Many technical challenges have to be solved in order to develop MCAO systems. One of them, related to its use on ELT's, is to find fast algorithms to perform the reconstruction at the required speed. For that reason we have been studying the application of the Fourier Transform Reconstructor (FTR) to MCAO. We use the Fourier Slice Theorem in order to reconstruct the atmospheric volume. For the simulations, Montilla *et al.*[10] have used a possible MCAO configuration for the E-ELT, as described for MAORY[12]. Figure 10 shows some results.

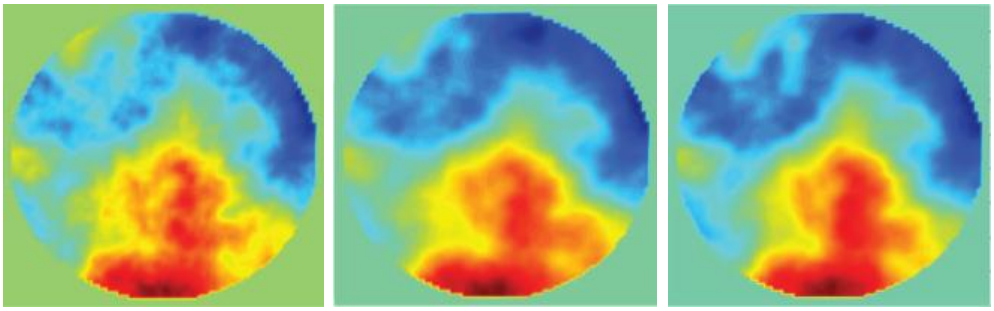

Figure 10. MAORY simulation. Left: reference wavefront. Center: reconstructed wavefront without optimization. Right: reconstructed wavefront with optimization. From Montilla *et al.*[10].

6. CONCLUSIONS.

We can summarize that plenoptic camera can measure the amplitude as well as the phase of the electromagnetic field. Also, that they couple nicely with the increasing capabilities, in term of number of pixels, of sensors. Where display technologies seem to ignore this increase, the plenoptic objective that we propose comes handy to convert this quantity of non-demanded pixels into a new ability for conventional cameras: to sense 3D. It is a remarkable characteristic of plenoptic cameras that most of the required changes involve processing rather than construction.

ACKNOWLEDGMENTS

This work has been partially funded by national R&D Program (Project AYA-13075) of the Ministry of Science and Innovation, by the Agencia Canaria de Investigación, Innovación y Sociedad de la Información (ACIISI) and by the European Regional Development Fund (ERDF).

REFERENCES

[1] Rodríguez-Ramos, J.M., *et al*., ES200800126 ES200600210 International Patent (2007,2009).
[2] Rodriguez-Ramos, J.M., *et al.*, "Adaptive Optics for Extremely Large Telescopes," Proc. AO4ELT (2009).
[3] Gasior, M. and Gonzalez, J.M. "Improving FFT Frequency Measurement Resolution by Parabolic and Gaussian Spectrum Interpolation," 11th Beam Instrumentation Workshop, (2004).
[4] Bolles, R.C., Baker, H.H. and Marimont, D.H. "Epipolar-plane image analysis: An approach to determining structure from motion," Int. Journal of Computer Vision, 1:7-55 (1987)
[5] Adelson, E. H. and Wang, J. Y. "Single lens stereo with a plenoptic camera," IEEE Transactions on Pattern Analysis and Machine Intelligence, 99-106, (1992)
[6] Ng, R., "Fourier slice photography," ACM Trans. Graph. 24, 3, 735-744 (2005)
[7] Marichal-Hernandez, J.G., *et al.*, "Fast approximate 4D:3D Radon transform, from lightfield to focal stack with O(N^4) sums," Proc. SPIE Electronic Imaging, San Francisco (2011)
[8] CAFADIS group, University of La Laguna *Side-by-side stereoscopic video showing the capability to refocus after acquisition of a plenoptic video camera*. http://pejeverde.lct.ull.es/cafadis/SPIE_DSS11/
[9] Rodríguez-Ramos, J.M., *et al*., "Wavefront and distance measurements using the CAFADIS camera, in Astronomical telescopes," Proc. SPIE Adaptive Optics Systems, Marseille (2008)
[10] Montilla, I., *et al.*, "Multiconjugate adaptive optics with plenoptic cameras and the Fourier Transform Reconstructor," Proc. SPIE Astronomical Telescopes, San Diego (2010).
[11] Clare, R.M. and Lane, R.G., "Wave-front sensing from subdivision of the focal plane with a lenslet array," J. Opt. Soc. Am. A 22 (2005)
[12] Diolaiti, E. *et al.*, "Towards the phase A review of MAORY, the multi-conjugate adaptive optics module for the E-ELT," Adaptative Optics for Extremely Large Telescopes, (2010)